CONF-951033--19

SAND95-1096C

TOWARDS A RELIABLE LASER SPRAY POWDER DEPOSITION SYSTEM THROUGH PROCESS CHARACTERIZATION

D. M. Keicher, J. L. Jellison, L. P. Schanwald and J. A. Romero
Sandia National Laboratories
Albuquerque, New Mexico 87185

D. H. Abbott
United Technologies Pratt and Whitney
East Hartford, Connecticut 06108

ABSTRACT

A series of experiments have been performed to characterize the laser spray powder deposition process. The goal of these experiments was to minimize the heat affected zone (HAZ) in the base substrate while obtaining a maximum build-up rate of the deposited material. Response surface models have been developed to achieve this goal. These models indicate that laser irradiance and component travel speed are both important factors to be considered in optimization of this process. These models suggest that a minimum HAZ can be obtained with a maximum material build-up height by maintaining with a slow travel speed. Although these models are useful in identifying significant factor and process trends, further refinement is required for practical use in industrial applications. Weighting of the response variables used in generating the models is being considered to improve the model robustness. High speed imaging of the deposition process suggests that the powder particle size and/or size distribution affects the stability of this process.

KEY WORDS: Lasers Processing, Powder Deposition, Response Surface Model.

INTRODUCTION

Since their development in the early 1960's, lasers have evolved from a novelty to a practical tool for industrial materials processing. In the last decade, laser cladding has proven to be a technology which satisfies industrial requirements for a variety of applications. Laser cladding of similar and/or dissimilar materials for improved wear properties, corrosion resistance, thermal barrier coatings, etc. has been investigated extensively[1-4]. Several groups have

DISCLAIMER

developed models to describe some of the physical phenomenon which occur during the laser cladding process[5,6]. Additional experiments have been performed to investigate such process interactions as the laser absorption by the metal powder[7], and to measure the surface temperature of the cladding layer during processing[8]. More recently, some groups have reported using a process similar to laser cladding for generating solid metal objects[9].

Although building solid metal geometries using laser powder deposition is a newly emerging technology, as far back as 1984 the concept existed[10] of using laser powder or wire deposition to rebuild and/or produce solid geometries. With the recent emphasis to improve the flexibility of production processes and move in the direction of agile manufacturing as an impetus, a broad effort to understand and enhance the performance of the laser powder deposition process has been initiated. Our effort focuses on using the laser spray deposition process for rework applications. For this application, minimizing the heat affected zone (HAZ) to an existing component is essential to insure the integrity and prolong the life of the existing hardware. The metallurgical properties of the deposition must be consistent with the base material. Developing a fundamental understanding of the laser powder deposition process will insure that a well-controlled laser spray fabrication process is achieved. In this study, the effects of the process input variables are analyzed to identify key process control parameters. From our empirical data, response surface models are then developed to be used in process optimization.

EXPERIMENT

Our objective for this study was to obtain a minimum HAZ in the substrate on which the powder was being deposited while maintaining a high density (>99%) deposit. To develop a fundamental understanding of the powder deposition process, a series of statistically designed experiments were developed to evaluate a factor space detailed below. The deposition experiments were performed on an 1800 W cw Nd:YAG laser with a three-axis positioning system. A schematic representation of the deposition experiment arrangement is shown in Fig. 1. The positioning stages were mounted inside a controlled atmosphere glove box operating at a nominal oxygen level of 2-3 parts per million. The glove box atmosphere was Ar. Both the substrate and the powder were Inconel® 625. The powder mesh size range was -80 to +325 mesh. Each test consisted of depositing 10 layers of powder onto the substrate in a line. The nozzle was moved away from the substrate a given increment after each pass. The powder flowed continuously through the nozzle during each test, but the laser beam was incident onto the substrate for travel only in one direction.

Our initial experiments were performed using a single point powder delivery nozzle which introduced powder into the laser beam from an off-axis direction at an angle approximately 40° from the beam optical axis. We quickly discovered, however, that this single point powder delivery nozzle provided inconsistent results. The powder feed unit used was a commercially available system used for thermal spray applications. As the powder feed pressure was increased, a low frequency pulsing of the powder feed rate occurred. When the pulsing occurred, a comb-like periodic structure was deposited on the sample substrate which would subsequently shadow the regions between the "teeth", inhibiting deposition in these regions. In addition, the deposition geometry would vary as a function of the component scan direction under the beam. This was clearly unacceptable for controlled experiments, so a new nozzle was designed. The new nozzle provided uniform deposition independent of travel direction and provided more consistent deposition layers even when pulsing of the powder stream was present. Figure 2 a shows the spray pattern achieved from this nozzle. In addition, a smaller powder feed unit (Fig. 2 b) was developed based on a former design[11] to provide more consistent powder feed results and eliminate pulsing effects.

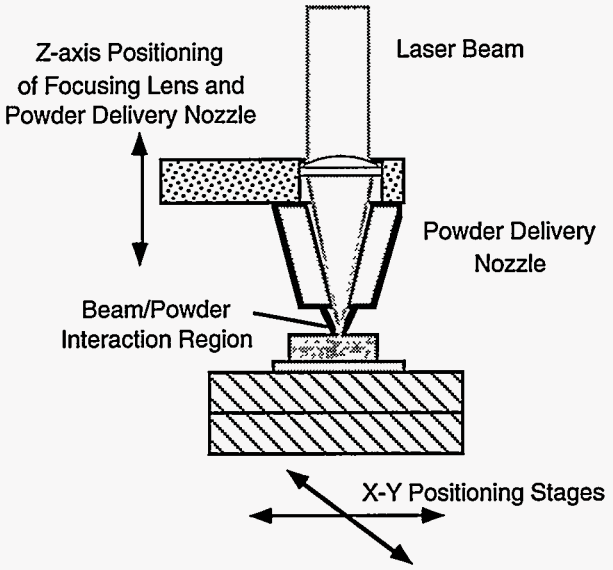

Figure 1. Configuration used in performing powder deposition experiments.

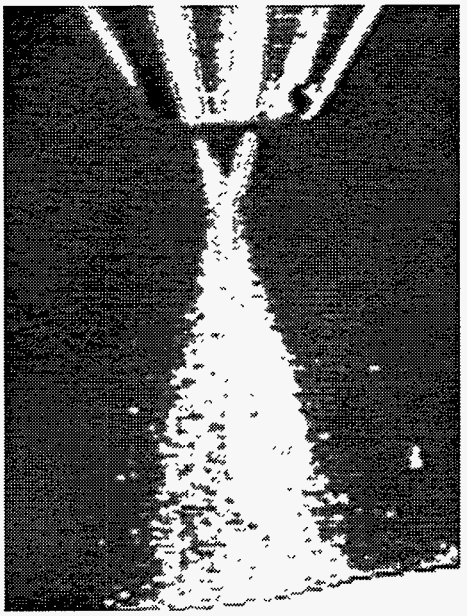

Figure 2. Photographs of (a) powder delivery nozzle showing spray pattern, (b) powder delivery unit developed for laser powder deposition process.

The factors space input variables considered for our experiments were: laser irradiance, travel speed, powder volume, powder velocity and z-axis increment between passes. The response variables examined were: the HAZ depth, the total height of the build-up and the density of the deposit. Several diagnostic techniques were used to measure the various input and response variables. A commercially-available Doppler velocimeter was used to determine the powder velocity from the nozzle. The beam irradiance values were calculated from measured values of the laser focused spot-size, obtained using a commercially-available beam diagnostic system, and power measurements obtained using a calorimetric detector. The powder volumetric flow rate was measured directly out of the nozzle by placing a bag over the end of the nozzle to capture the sprayed powder for a predefined time period. The bags containing the powder were

subsequently weighed and the measured values were used to calculate values for the powder volumetric flow rate. The component and nozzle travel increments and speeds were set at the CNC positioning controller for each test. In addition to these response variables, infrared and high speed imaging techniques were used to monitor the deposition process and provide insight into the controlling physics of the process.

The conditions used in the experiment test matrix are given in Table 1. The aim points were identified from parameters which easily implemented, i.e. laser power, gas pressure, etc., however, the actual values varied slightly from the aim points.

After processing, each deposition was metallographically cross-sectioned transverse to the deposition direction. Photomicrographs were taken from which the depth of the melt region below the original surface was measured. For this set of experiments, the melt region was easy to discern. The HAZ was defined to be the region below the original substrate surface to which melting occurred. To insure that the melt region was a valid measure of the HAZ, high magnification optical photomicrographs of the melt-zone/substrate interface were also taken to observe any intergranular melting or other microstructural changes which might have occurred. The build-up height was simply taken to be the distance from the original substrate surface to the maximum point on the deposition region. All deposits exhibited a similar convex semicircular shape.

Table 1. Process variables considered for statistically designed experiments.

Input Variable	Low	Medium	High
Laser Irradiance (W/mm^2)	345	549	774
Travel Sped (mm/s)	8.47	21.17	33.9
Z-Axis Increment	.127	.229	.38
Powder Volume (gm/min.)	1.785	2.418	3.06
Carrier Gas Pressure (Pa)	$1.38x10^5$	-	$2.07x10^5$
Powder Velocity (mm/s)	5000	-	6500

An intensified and gated high speed digital imaging system was used to observe the beam/powder interaction in the deposition region. A schematic representation of the experimental arrangement is given in Fig. 3. To view through the intense laser plume, a 150 mW, 690 nm wavelength diode laser was used as an illumination source and a laser line filter at this wavelength was placed in front of the lens. For the high speed video, two different powder sizes were used to see the effect of powder size on the performance of the process. The powder size distributions for the two powders were: -80 to +325 mesh for the larger powder size and -325 mesh for the smaller powder size. The framing rate on the camera was 2000 pictures per second and a gate width of 50 μs was used at ~50x magnification. The high speed video results were also used to visually identify whether significant heating of the powder particles occurred prior to impingement into the deposition melt zone.

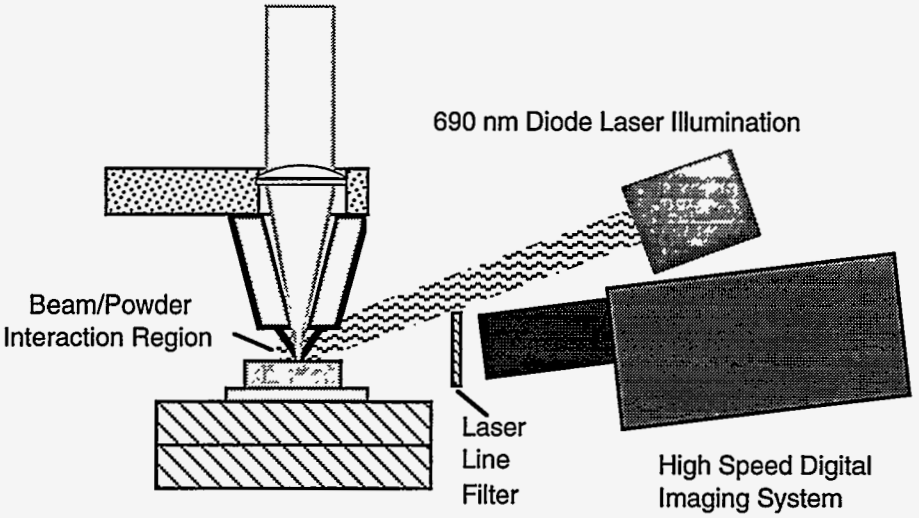

Figure 3. Schematic representation of arrangement used in high speed imaging of powder deposition process.

RESULTS, ANALYSIS AND DISCUSSION

Complete melting of the powder occurred for all the tests performed during these experiments. In addition, epitaxial growth of the deposited material occurred across the deposition layer boundary in nearly all cases. This structure is represented in Fig. 4 (a) for the deposition conditions: 345 W/mm^2 irradiance, 8.47 mm/s travel speed, 1.9 gm/min. powder volume, 1.38x10^5 Pa. gas pressure and 0.381 mm/pass z-axis increment. Figure 4 (b) shows the melt zone/substrate interface for the highest energy input parameters used in these experiments (774 W/mm^2 irradiance, 1.9 gm/min. powder volume, 1.38x10^5 Pa carrier gas, 8.47 mm/s travel speed, 0.254 mm/pass z-increment). As can be seen from this photograph, there was very little intergranular melting in the substrate region, and no other significant microstructural changes in the grain size, shape and density. The intergranular melting which has occurred (indicated by arrow), goes into the substrate only a fraction of the substrate grain size. Therefore, the assumption that the melt zone is representative of the HAZ is valid.

Figure 5 shows the HAZ depth into the substrate as a function of the build-up height. The HAZ depth varied from a minimum of 0.048 mm to a maximum of 0.273 mm. The build-up height varied from a minimum of 0.071 mm to a maximum of 1.730 mm. The data sets are identified by the laser power and travel speed associated with each condition. As shown in Fig. 5, the melt depth tends to increase with increasing laser power though effect saturates at 220 W. There is, clearly, a great deal of overlap in the melt depth conditions for the intermediate and high power parameters. At all power levels, there is a significant increase in build-up of the deposited material as the component travel speed is decreased with at most a modest increase in the melt depth. In general, the trend from this analysis suggests that the penetration into the substrate occurs early on in the deposition process. If the part is scanned under the beam at a slow rate of speed, the powder is given time to build while little more penetration occurs. Similarly, if the substrate is scanned under the beam at a high rate of speed, the penetration into the substrate is affected little but the build-up is inhibited. All of the data in Fig. 5 at a build-up height of greater than 1 mm occurred at a slow scan speed. In any case, it is logical that the

minimum penetration into the substrate will occur when the irradiance is low yet sufficient to incur complete melting.

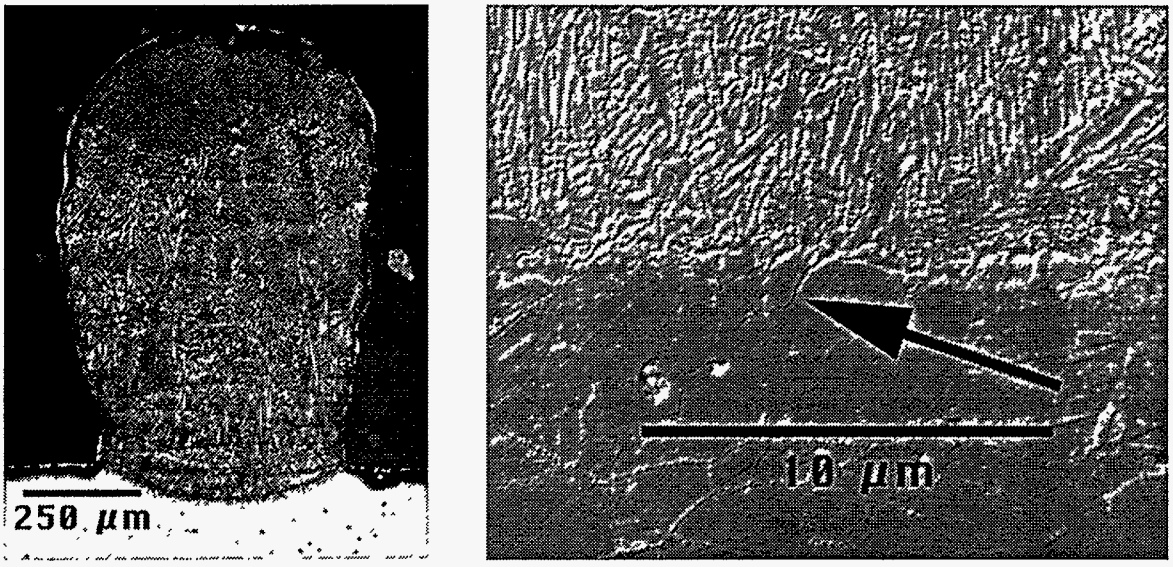

(a) (b)

Figure 4. Photomicrographs showing a) epitaxial growth for laser deposited materials:, b) melt zone/substrate region.

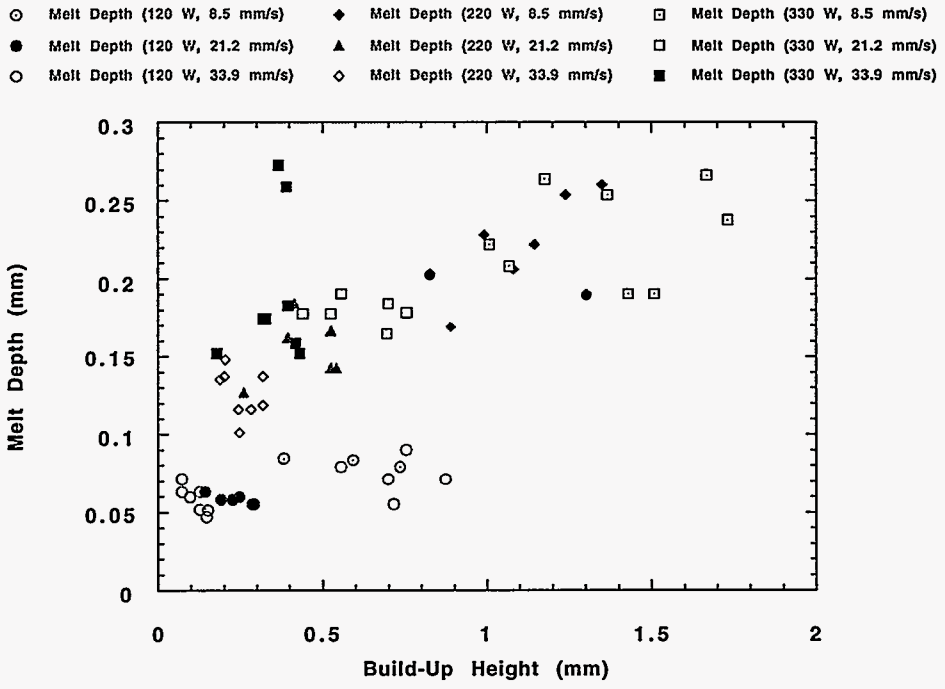

Figure 5. Measured results for melt depth and build-up height from experiment test matrix.

Visual examination of the photomicrographs exhibited no obvious signs of porosity in the deposited material. The cross-sections are similar in appearance to those observed in laser

welds. Although there are no obvious defects in the deposited materials, microprobe analysis is presently being performed to quantify the percentage of porosity in the deposition as compared to the substrate. This analysis will also identify differences in composition between the deposited material and the original substrate to insure that none of the elements within the deposition layers was preferentially vaporized. This could affect the integrity of the deposited material. No sign of cracking within the deposited materials was noted.

The data sets generated were used to develop response surface models for the laser spray deposition process in order to identify significant factors for process optimization. The analysis was performed for both the melt depth and the build-up material height response variables. A third composite response surface variable was developed using the ratio of the measured melt depth to the measured build-up height. In all cases, the data sets obtained were found to possess a normal distribution, and statistically significant factors were identified for each of these models. The analysis also determined the statistical significance of the fits.

Analysis of the response variable for melt depth into the substrate determined that the significant factors in this model are the laser irradiance, I, and the travel speed, v. The equation for the melt depth is then given by:

$$MeltDepth = -0.2111 + 0.00125I - 0.00389v - 10^{-6} I^2.$$

A contour plot for the melt depth as a function of irradiance and speed is given in Fig. 6. As expected, the minimum melt depth is achieved at the lower irradiance values and increases with increasing irradiance, and the maximum melt depth is achieved at the highest irradiance with a low travel speed. For the low to intermediate irradiance regions, the contour plot also shows that the melt depth is highly dependent on the irradiance and decreases slowly with increased travel speed.

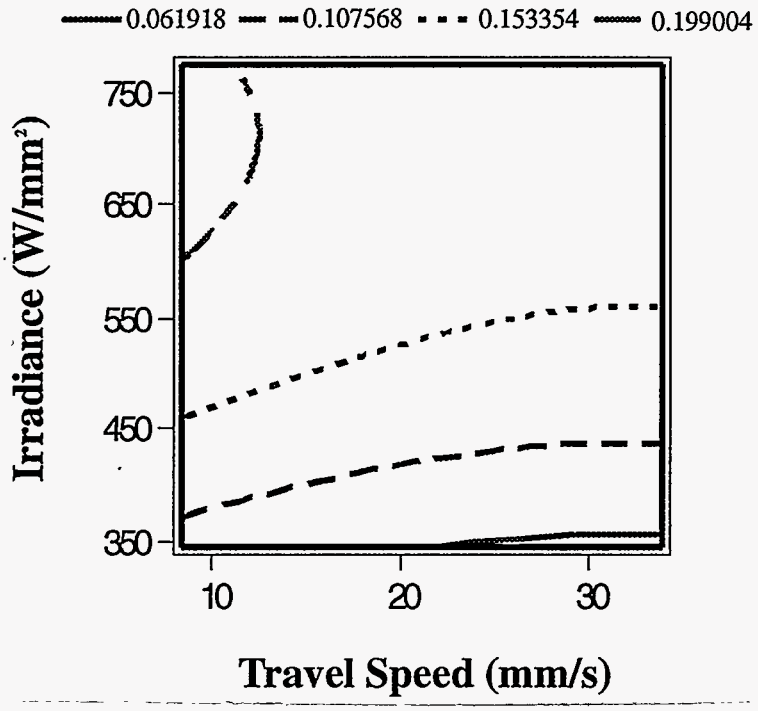

Figure 6. Response surface contour plot of melt depth into the substrate as a function of irradiance and travel speed.

A second response surface model for the material build-up height suggests that the significant factors for this test are again the laser irradiance, I, and the part travel speed, v. The build-up height is given as:

$$BuildUp = 0.508 + 0.00247I - 0.063v + 0.00108v^2 - 10^{-6}I^2 - 2.1\times10^{-5}Iv.$$

A contour plot of this model as a function of irradiance and travel speed is given in Fig. 7. This contour plot shows that the build-up height of the deposited material is highly dependent on the travel speed at high irradiance, but starts to depend on irradiance also at low values of irradiance. At high travel speed the build-up is proportional to irradiance but remains relatively flat for irradiance above 550 W/mm^2. As the travel speed is decreased below 20 mm/s the rate of material build-up increases significantly, however.

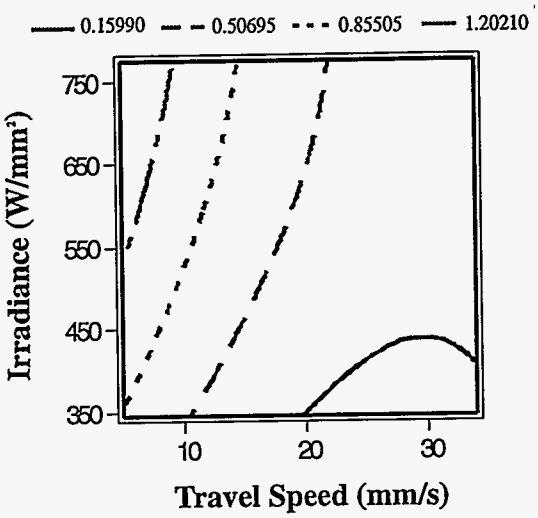

Figure 7. Response surface contour plot of response surface for the material build-up height as a function of irradiance and travel speed.

It is obvious that reducing the laser irradiance at constant travel speeds reduces the melt depth into the substrate. However, this also reduces the build-up rate. To achieve a minimum melt depth into the substrate and yet obtain reasonable build-ups, the third response variable, the ratio of the melt depth to the build-up height, was considered. In this case a small value for the response variable would indicate a condition where the melt depth was minimized with a large build-up rate. Each of the response variables used in creating the third response variable were weighted equally in this study. It is likely that the results would shift if different weighting factors were used for the melt depth or build-up height. However, for our initial study we were interested in characterizing the process.

This analysis showed that the irradiance and speed were again significant variables, which is consistent with previously reported results[12]. However, the powder volume, P_v, and z-increment, z, values were also determined to be significant. The equation for the melt depth to build-up height ratio is given as:

$$\frac{MeltDepth}{BuildUp} = -0.3027 + 0.0017I + 0.0184v - 0.0908P_v + 0.3124z - 10^{-6}I^2.$$

A contour plot of the ratio variable as a function of irradiance and travel speed is given in Fig. 8 (a). As can be seen from this plot, the response surface indicates a reduced value for the ratio as the travel speed is reduced. Minimum values are obtained for each of the contour lines for low and high irradiance values. Since the data in Fig. 5 shows that the minimum melt depth is achieved for the low irradiance values, this contour plot (Fig. 8 (a)) would suggest that the ratio response variable considered is influenced by the large build-up rate which occurs at the higher irradiance value. We can clearly see that optimum conditions for obtaining a minimum melt depth with good build-up height occur at a slow travel speed which is less clearly seen in Fig. 5.

Also shown are contour plots for the melt depth/build-up response variable as a function of irradiance and powder volume Fig. 8 b and irradiance and the z-increment (Fig. 8 (c)). Figure 8 (b) indicates that increasing the powder volume would lead to a decrease in the melt depth/build-up ratio. As shown in Figs. 5 and 6, the melt depth does not change significantly with increased speed at low to intermediate irradiance values. This would suggest that an improvement in the material build-up per pass could be gained by increasing the powder volumetric flow rate to the deposition region. Figure 8 (c) suggests that the ratio could be decreased by reducing the increment of the z-axis. For these experiments, the largest build-up per pass layer was 0.17 mm. The increment used in these tests for the z-axis is larger than this maximum deposition rate in all but the minimum case (see Table 1). From this result one might conclude that the process could improved by matching the z-axis increment to that of the build-up rate.

Finally, high speed imaging using filtered illumination allowed us to visualize the molten powder deposition region to develop a qualitative understanding of the material build-up. For both particle sizes, it appears that particles do not become molten until they are actually injected into the molten metal puddle in the deposition region. For the larger particle size, the molten puddle was very energetic and unstable. For the smaller particle size distribution, the melt puddle appeared to be much more stable and well behaved. For the larger powder size distribution, the particle size was a significant fraction of the deposition region depth. Directing the particles into the molten deposition region would be analogous to throwing small pebbles into a pond. The fine pebbles disturb the surface of the pond, but do not cause gross material motion. In contrast, dropping a very large boulder into the pond displaces a significant volume of liquid. The larger displacement of the melt pool coupled with the larger particle size distribution is likely the cause of the instabilities in the deposition melt region. In any case, these results suggest that further studies need to be performed to identify the effects of particle size on the powder deposition process.

CONCLUSIONS

We have developed response surface models based on empirical data which can used to optimize the laser spray deposition process to minimize the HAZ or maximize the deposition build-up height. A further response surface model has been developed to minimize the HAZ while obtaining a maximum build-up rate. This third model, however, requires further refinement for practical use. These statistically based models indicate the importance of the laser irradiance and component travel speed on the process outcome. Our results suggest that maintaining a slow travel speed allows the optimum material build-up rate to be achieved with a minimum HAZ. High speed imaging results show that the powder particle size and/or size distribution has a significant effect on the stability of the molten deposition region. Further studies are suggested to assess the significance of this effect on process stability.

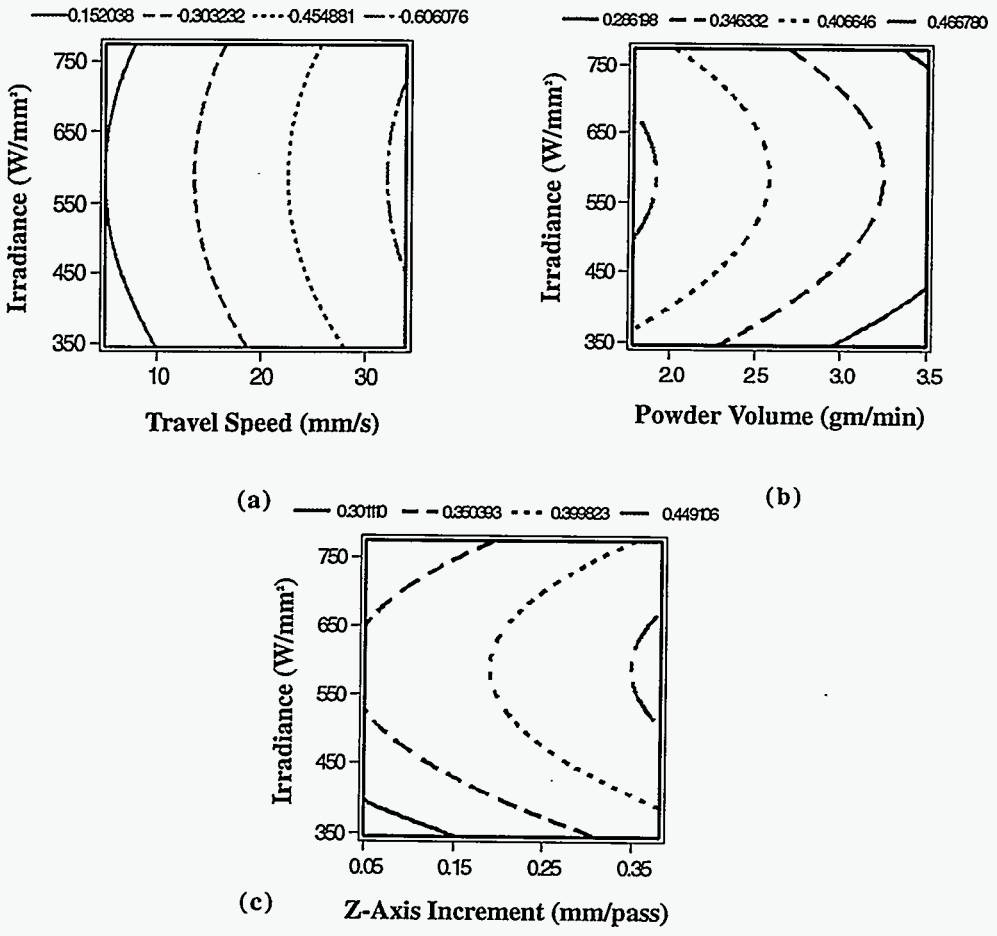

Figure 8. Response surface contour plot for ratio of the measured melt depth to build-up height as a function of irradiance and: (a) travel speed, (b) powder volume and (c) z-increment per pass.

ACKNOWLEDGMENTS

We would like to thank Francisco Jeantette and Peter Jeantette for their assistance in performing these experiments. We would also like to thank Jerry Knorovsky for his insightful input and technical review of this paper. Our thanks also goes to Ray Cote, Mark Smith and Rich Neiser of the Thermal Spray Group at Sandia for their guidance with powder spray processes.

*This work was performed at Sandia National Laboratories supported by the U. S. Department of Energy under contract number DE-AC04-94AL85000.

REFERENCES

REFERENCES

1) A. Frenk and J. D. Wagniere, "Laser Cladding with Cobalt-Based Hardfacing Alloys," J. Phys. IV, **1** (1991) p 65.

2) R. Subramanian, S. Sircar and J. Mazumder, "Laser Cladding of Zirconium on Magnesium for Improved Corrosion Properties," J. Mater. Sci. **26** (1991) p 951.

3) K. M. Jasim, R. D. Rawlings and D. R. F. West, "Thermal Barrier Coatings Produced by Laser Cladding," J. Mater. Sci. **25** (1990) p 4943.

4) J. De Damborenea and A. J. Vazquez, "Laser Cladding of High-Temperature Coatings," J. Mater. Sci. **28** (1993 p 4775.

5) S. Sircar, K. Chattopadhyay and J. Mazumder, "Nonequalibrium Synthesis of $NbAl_3$ and Nb-Al-V Alloys by Laser Cladding: Part I. Microstructure Evolution," Metall. Trans. A **23A** (1992) p 2419.

6) J. Mazumder and A. Kar, "Solid Solubility in Laser Cladding," J. Met. (Feb. 1987) p 18.

7) Y. Kizaki, H. Azuma, S. Yamazaki, H. Sugimoto and S. Takagi, "Phenomenological Studies in Laser Cladding. Part I. Time-Resolved Measurements of the Absorptivity of Metal Powder," Jpn. J. Appl. Phys. **32** (1993) p 205.

8) Y. Kizaki, H. Azuma, S. Yamazaki, H. Sugimoto and S. Takagi, "Phenomenological Studies in Laser Cladding. Part II. Thermometrical Experiments on the Melt Pool," Jpn. J. Appl. Phys. **32** (1993) p 213.

9) J. L. Koch and J. Mazumder, "Rapid Prototyping by Laser Cladding," ICALEO '93 Proc. **77** (1993) p 556.

10) Pratt and Whitney Patent

11) Personal Communication with R. O. Cote, Sandia National Laboratories Thermal Spray Group, 694 to 9-94..

12) C. Xin and T. Zhenyi, "Maximum Thickness of the Laser Cladding," Key Eng. Mater. **46** (1990) p 381.